

Transient translational quiescence in primordial germ cells

Nathalie Oulhen¹, S. Zachary Swartz^{1,2}, Jessica Laird¹, Alexandra Mascaro¹ and Gary M. Wessel^{1,*}

ABSTRACT

Stem cells in animals often exhibit a slow cell cycle and/or low transcriptional activity referred to as quiescence. Here, we report that the translational activity in the primordial germ cells (PGCs) of the sea urchin embryo (*Strongylocentrotus purpuratus*) is quiescent. We measured new protein synthesis with O-propargyl-puromycin and L-homopropargylglycine Click-iT technologies, and determined that these cells synthesize protein at only 6% the level of their adjacent somatic cells. Knockdown of translation of the RNA-binding protein Nanos2 by morpholino antisense oligonucleotides, or knockout of the Nanos2 gene by CRISPR/Cas9 resulted in a significant, but partial, increase (47%) in general translation specifically in the PGCs. We found that the mRNA of the translation factor eEF1A is excluded from the PGCs in a Nanos2-dependent manner, a consequence of a Nanos/Pumilio response element (PRE) in its 3'UTR. In addition to eEF1A, the cytoplasmic pH of the PGCs appears to repress translation and simply increasing the pH also significantly restores translation selectively in the PGCs. We conclude that the PGCs of this sea urchin institute parallel pathways to quiesce translation thoroughly but transiently.

KEY WORDS: Metabolism, Primordial germ cells, Sea urchin, Translation

INTRODUCTION

Primordial germ cells (PGCs) are the newly formed germ line of the embryo. These cells are specified during early development, migrate to the gonad and then proliferate to form the gonial stem cells of the future eggs and sperm of the adult. In animals for which the PGCs form early in development, usually by acquired maternal determinants (e.g. flies, nematodes, zebrafish), their specification precedes gastrulation and the PGCs become quiescent in terms of cell division and transcription (Williamson and Lehmann, 1996). These cells remain less active than their somatic siblings until tissue rearrangements and organogenesis begin, when they then migrate to the gonad and increase cell division and transcriptional activity.

Echinoderms are sister to the Chordates; in the sea urchin *Strongylocentrotus purpuratus*, the primordial germ cells originate at the 5th cell division (32 cell stage) by two sequential asymmetric divisions of the small micromeres. This early segregation from a somatic fate creates a unique challenge to the embryo; it is one of the earliest germ lines to form in terms of cell cycle number, and how it deals with this disparity in timing of development is of logistical significance. The cell cycle of the sea urchin PGCs is immediately

slowed; the cells divide only once more by the end of gastrulation. Associated with the slow cell cycle, these cells also have low transcriptional activity and retain a large proportion of their maternally derived mRNA (Wessel et al., 2014). These changes occur in the midst of sibling somatic cells that are rapidly dividing to form over 1500 cells, which display high transcriptional activity and dynamic transcriptional changes, dramatic turnover of maternal mRNA and protein, and lively cell and tissue reorganization. We document here that the PGCs also quiesce their protein synthesis and do so transiently in part due to the selective expression of the RNA binding protein Nanos2. We have thus named this process transient translational quiescence (TTQ).

Nanos was first identified in *Drosophila* as a translational repressor (Cho et al., 2006; Irish et al., 1989). It functions through its interaction with Pumilio, which binds RNAs containing a conserved motif usually found in the 3'UTR of mRNAs; this motif is referred to as the Pumilio response element (PRE) (Sonoda and Wharton, 1999; Wharton and Struhl, 1991). Only a few genes have been identified as Nanos/Pumilio targets: *cyclin B* (Asaoka-Taguchi et al., 1999; Dalby and Glover, 1993; Kadyrova et al., 2007; Lai et al., 2011), *hid* (Hayashi et al., 2004; Sato et al., 2007), *hunchback* (Murata and Wharton, 1995; Wreden et al., 1997), *fem3* (Ahringer and Kimble, 1991; Zhang et al., 1997), *VegT* (Lai et al., 2012) and *CNOT6* (Swartz et al., 2014). In the sea urchin *Strongylocentrotus purpuratus* (the purple sea urchin), three nanos orthologs are present in its genome, but *SpNanos2* (mRNA and protein) is the only Nanos that accumulates specifically in the PGCs at the blastula stage when the quiescence phenotype is detected (Juliano et al., 2010). Our data show that Nanos2, by regulating the mRNA coding for eEF1A, is responsible in part for the dramatic translational quiescence seen in these early born PGCs.

RESULTS

Protein synthesis is transiently quiescent in the PGCs

In contrast to radioactive amino acids or specific antibodies against translational factors that limit a direct and specific measurement of the translational activity throughout the development, modified chemistries now enable direct imaging and quantification of protein synthesis at high resolution *in situ*. We tested both a methionine analog, HPG (homopropargylglycine), and a modified translational inhibitor, the OPP (O-propargyl-puromycin) (Starck et al., 2004), and found highly compatible results in both. Both reagents are taken up by cells and are incorporated into the nascent peptide chain for covalent labeling, even after fixation of the embryo. In the sea urchin, the overall rate of protein synthesis is low in unfertilized eggs due to a low cytoplasmic pH but is stimulated rapidly following fertilization, independent of mRNA transcription and ribosome biogenesis (Epel, 1967; Cormier et al., 2001; Brandhorst, 1976). This nearly instantaneous activation can be mimicked by increasing the cytoplasmic pH of the egg from pH 6.8 to pH 7.3 with ammonium chloride (Epel, 1967). As expected, protein synthesis was not detectable in unfertilized eggs by OPP incorporation, but the embryos rapidly revealed robust activity (Fig. S1). This

¹Department of Molecular and Cell Biology and Biochemistry, Brown University, 185 Meeting Street, Providence, RI 02912, USA. ²Whitehead Institute for Biomedical Research, MIT, Nine Cambridge Center, Cambridge, MA 02142, USA.

*Author for correspondence (gary_wessel@brown.edu)

 G.M.W., 0000-0002-1210-9279

synthetic activity was sensitive to protein synthesis inhibitors, demonstrating the specificity of this component to measure translation *in situ* in this embryo. To test the translational activity of the PGCs throughout development, these cells were co-labeled with a Vasa antibody to definitely identify the PGCs. Translational activity in the PGCs was found to be significantly reduced ($6\% \pm 2.7$) relative to its sibling somatic cells in the animal pole, and is transient – these cells return to normal levels of translational output following gastrulation (i.e. comparable to its precursor siblings and to neighboring cells) within 72 h post-fertilization, demonstrating a transient quiescent activity (Figs 1 and 2). HPG yields similar results (Fig. S2) and, importantly, these *in situ* results are concordant with the use of radioactive amino acid reagents in this animal (Karp and Weems, 1975). Thus, three different chemistries yield the same biological result. In early dividing cells of the embryo, newly synthesized protein accumulated robustly in the nuclei, a consequence of the significant early stage synthesis of histone proteins (Davidson, 1976). They are translated and incorporate HPG or OPP in the cytoplasm, and then shuttle rapidly to the nucleus, leading to a high nuclear signal (Fig. 1).

Nanos2 is required for the transient translational quiescence in the PGCs

The Nanos2 protein is only detectable by immunolocalization in the PGCs at blastula and gastrula stages (Juliano et al., 2010; Fig. S3), which correlates precisely with the transient translational quiescence (TTQ) phenotype. To test the function of Nanos2 in TTQ, we knocked-down Nanos, using a previously characterized Nanos morpholino to reduce Nanos protein to undetectable amounts (Juliano et al., 2010) and learned that Nanos2 does not influence translation in somatic cells, but dramatically increased the translational activity in the PGCs to 47% that of the somatic cells (Fig. 2). Importantly, vegetal plate cells adjacent to the PGCs also have reduced translational activity relative to other somatic cells (50%), but they maintain their level of translation independently of

Nanos protein. This Nanos-independent mechanism observed in the vegetal cells is currently under investigation.

Similar results were obtained when Nanos2 function was inactivated by using the CRISPR/Cas9 approach (Fig. 3). To first test the efficiency of this CRISPR/Cas9 method, we targeted genes of the pigment cell pathway, resulting in albinism in the larvae in over 95% of the embryos (Oulhen and Wessel, 2016; and data not shown). We then designed multiple gRNAs targeting the single exon Nanos2 gene and monitored efficiency of Nanos2 inactivation functionally, by the accumulation of Vasa protein in the PGCs in gastrulae (Juliano et al., 2010). The CRISPR/Cas9 directed Nanos2 inactivation led to high-efficiency mutations (80% of the embryos had 100% of their nuclei mutated) and loss of Vasa expression in the PGCs (Fig. 3). Importantly, targeted gene inactivation of Nanos2 also functionally increased protein synthesis specifically in the PGCs (Fig. 3J). Altogether, these data indicate that Nanos2 is an essential, though not complete, regulator of the TTQ phenotype.

Nanos2 targets the essential translation factor eEF1A to cause low translation in the PGCs

To identify potential mechanistic candidates involved in the TTQ, we used a previously published transcriptomic dataset (Swartz et al., 2014). *eEF1A* mRNA, which codes for a translation elongation factor, was identified as a transcript that was downregulated in the PGCs (Swartz et al., 2014). When bound to GTP, the protein eEF1A delivers the aminoacylated-tRNA to the A site of the ribosome (Merrick, 2000). Two orthologs of eEF1A exist in mammals, although only one is present in the *Sp* genome (SPU 000595) (Morales et al., 2006), making it an essential translation factor. By fluorescence *in situ* hybridization, *eEF1A* mRNA is found at detectable levels throughout early development (data not shown), but is depleted from the PGCs at blastula and gastrula stages (Fig. 4). The protein is also present ubiquitously in early stages of development, but is rapidly excluded from the PGCs between blastula and early gastrula (Fig. S4). Of significance, we learned that

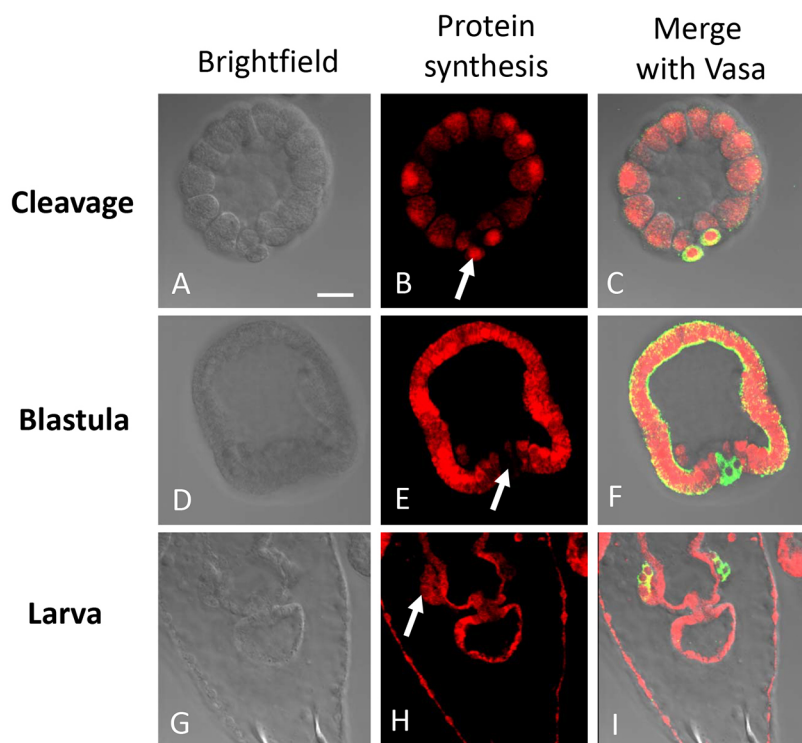


Fig. 1. Translation is transiently reduced in the PGCs at blastula stage. At different time points after fertilization: 5.5 h post fertilization at cleavage stage (A–C), 18 h (blastula stage) (D–F) or 3 days (larva stage) (G–I). Embryos were treated with OPP. Protein synthesis is represented in red and Vasa antibody (green) is used as a marker to localize the PGCs. Arrows indicate PGCs and transient quiescence. Approximately 100 embryos were visualized and representative embryos are presented. Scale bar: 20 μ m.

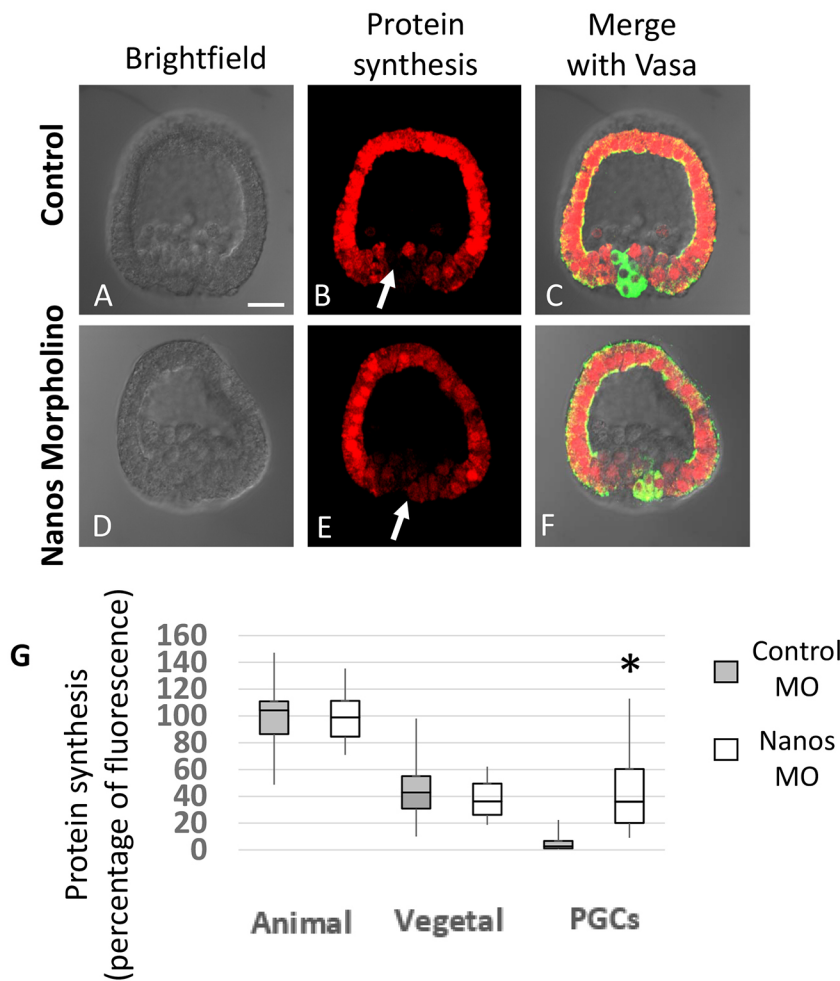


Fig. 2. Nanos is essential to maintain a translational quiescence in the PGCs. (A-F) Fertilized eggs were injected with either a control morpholino or Nanos morpholino, and treated with OPP at blastula stage (18 h post-fertilization) to visualize protein synthesis (red). Vasa immunofluorescence (green) indicates the location of the PGCs (arrows). Approximately 100 embryos were visualized and representative embryos are presented. Scale bar: 20 μ m. (G) For each morpholino, the intensity of OPP was measured in the animal pole, the vegetal pole and the PGCs; the results are presented as percentages compared with the animal pole. Thirty-five blastulae were quantified for the control morpholino and 29 for the Nanos morpholino. Significance was assessed for each area of the blastula between control and Nanos morpholino using Student's *t*-test (* P <0.001).

the morpholino targeting *Nanos2* mRNA resulted in the accumulation of *eEF1A* mRNA specifically in the PGCs (Fig. 4), coincident with the increased translational activity. The 3' UTR of *eEF1A* contains a putative PRE sequence (TGTAAT), suggesting that it is a Nanos/Pumilio target. To test whether the Nanos2-dependent repression of *eEF1A* mRNA accumulation relied on this element, a morpholino complementary to the *eEF1A* PRE was injected to block its interaction with the Nanos/Pumilio complex (Fig. 5), an approach used effectively for other mRNAs containing PREs (Swartz et al., 2014). The results show that the PRE is required to exclude *eEF1A* mRNA from the PGCs; in the presence of the PRE-blocking morpholino, a nearly fourfold increase in protein synthesis occurred specifically in the PGC (Fig. 5). Of note, even though *eEF1A* mRNA is present throughout the embryo, and the morpholino was injected in the egg, *eEF1A* mRNA was not significantly affected in the somatic cells (100% in the control morpholino, versus 94% in the PRE morpholino). Thus, exclusion of *eEF1A* from the PGCs seems dependent upon the presence of Nanos.

To test the function of *eEF1A* in the TTQ, we ectopically expressed the protein throughout the embryo (Fig. S5). Overexpression of *eEF1A* in the blastula [using a 3' UTR lacking the PRE, and thus insensitive to Nanos2 (Oulhen et al., 2013)] does not affect the level of protein synthesis in the somatic cells (Fig. 6). However, the translational activity in the PGCs increased significantly (to 17%) and specifically in the PGCs. Altogether, these data indicate that regulating *eEF1A* expression, through

Nanos2, is essential to maintain the TTQ in the PGCs. Clearly, though, *eEF1A* by itself is not the sole linchpin regulating TTQ in a Nanos2-dependent fashion. Indeed, scanning the transcripts depleted from the PGCs during TTQ (Swartz et al., 2014) reveals several other candidates that may be regulated similarly to *eEF1A* and contribute to the TTQ phenotype.

Both cytoplasmic pH and mitochondrial activity are also reduced in the PGCs

Nanos2 is an essential, but not the sole, regulator of TTQ. Indeed, protein synthesis in the PGCs is decreased relative to its neighboring somatic cells even before the exclusion of *eEF1A* (Fig. 7). Moreover, the mRNA coding for the ADP/ATP translocase 1 was also identified as downregulated in the PGCs (Swartz et al., 2014) and fluorescence *in situ* hybridization shows a depletion of this RNA in the PGCs, during gastrulation (Fig. 8). We note that the 3' UTR in the mRNA of this essential mitochondrial factor does not contain a consensus PRE, suggesting a Nanos/Pumilio-independent mechanism of mRNA exclusion from the PGCs.

Furthermore, the activity of the mitochondria is also transiently reduced in the PGCs in late blastula and gastrula (Fig. 8). The mitochondria in the PGCs have only 1.7% (\pm 2.3%) the activity of the adjacent somatic cells. This activity is reduced due to a decrease in the number and a decrease in the activity of mitochondria in the PGCs (Fig. S6). Inactivation of the mitochondria could lead to a shift in metabolism from oxidative phosphorylation to a glycolytic dependence, resulting in acidification of the cytoplasm. Sea urchin

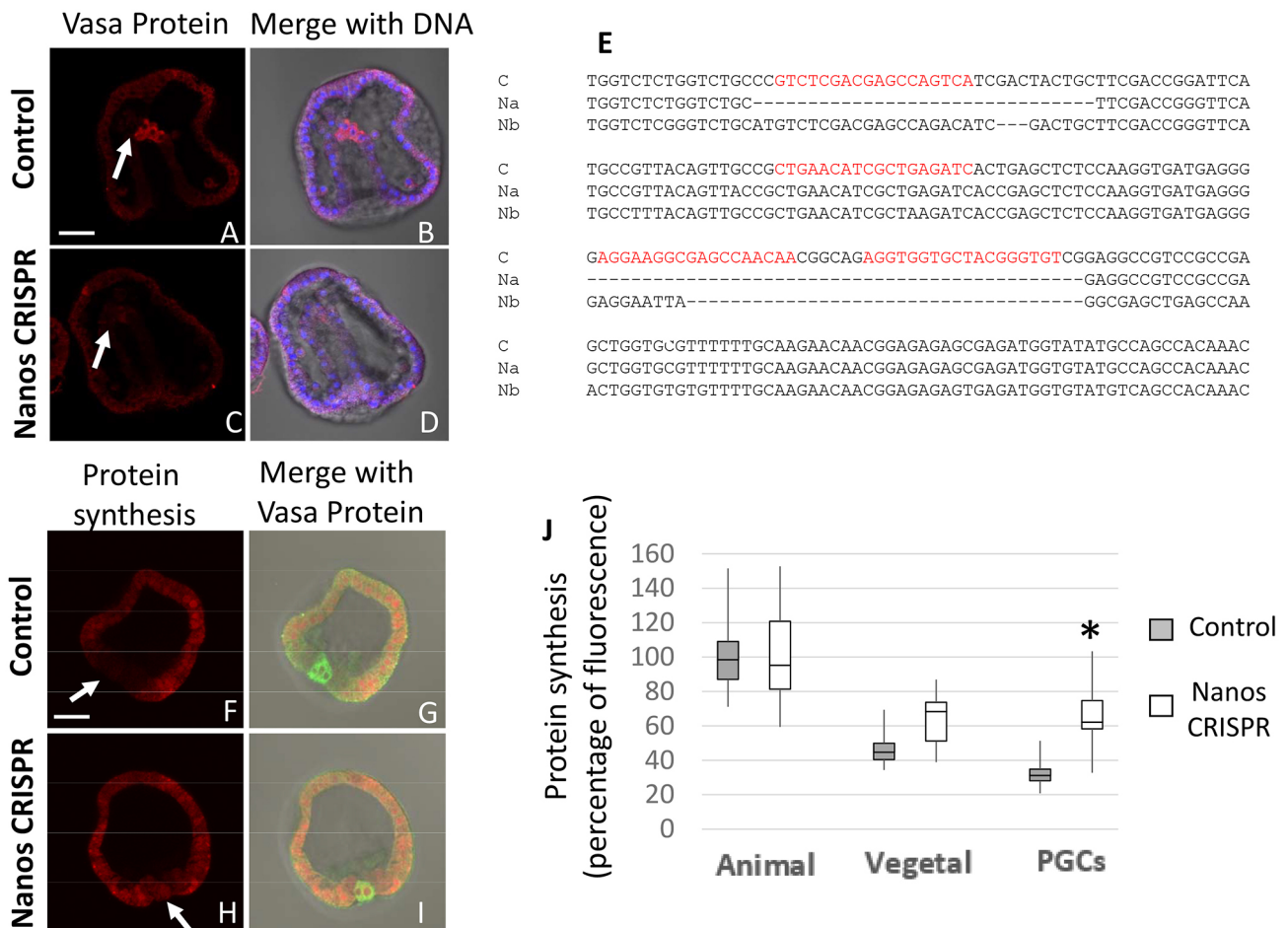


Fig. 3. The CRISPR approach supports the function of Nanos in the TTQ. Fertilized eggs were injected with either the Cas9 mRNA alone (control) or the Cas9 mRNA mixed with all four gRNAs directed against Nanos (Nanos CRISPR). These injected embryos were used to test the expression of Vasa protein in the PGCs (arrows, red) during gastrulation (A-D). DNA was labeled with Hoechst (blue). Sp Nanos2 gene was sequenced after genomic DNA extraction (E). Embryos injected with the Nanos CRISPR (Na and Nb) show several representative examples of mutations and deletions, compared with the control (C). One of the embryos even had a 117 nucleotide excision (not shown). Only a partial sequence of Sp Nanos2 is shown here, corresponding to the region targeted by the gRNAs (represented in red). (F-I) Finally, some injected embryos were also treated with HPG at blastula stage (18 h post-fertilization) to visualize protein synthesis (red). Vasa immunofluorescence (green) indicates the location of the PGCs (arrows). (J) For each embryo, the intensity of the HPG was measured in the animal pole, the vegetal pole and the PGCs; the results are presented as percentages compared with the animal pole. Ten blastulae were quantified for the control and 10 for the Nanos CRISPR. Significance was assessed for each area of the blastula between control and Nanos CRISPR with the use of Student's *t*-test (**P*<0.001). (A-D, F-I) Approximately 100 embryos were visualized and representative embryos are presented. Scale bars: 20 μ m.

eggs have a slightly acidic cytoplasm (pH 6.8) that represses translation (Epel, 1967), so we used the same strategy used in eggs to determine whether the proposed acidification was a functional contributor to translational quiescence in the PGCs. We incubated blastulae with cell-permeant ammonium chloride, which is known to activate protein synthesis in a pH-dependent process in the egg; this treatment significantly increased the translational activity in the PGCs, compared with the somatic cells, without affecting the level of eEF1A mRNA in the PGCs (Fig. S7). Thus, the TTQ mechanism in this embryo appears to be regulated by at least two parallel pathways: a Nanos2-dependent transcript degradation of essential translation factor(s); and a metabolic shift leading to changes in cellular physiology in the PGCs.

DISCUSSION

Quiescence is a shared character of many stem cells. The paradigmatic quiescent stem cell is the hematopoietic lineage, which is maintained at a low cell cycle, but can be stimulated to form new blood cells in response to signaling (Valcourt et al., 2012;

Nakamura-Ishizu et al., 2014). Recent research has documented that many tissues in human have quiescent stem cells (Rezza et al., 2014), including skeletal muscle (Boosanay et al., 2016; Fukada et al., 2007), the hair follicle (Morris et al., 2004; Goldstein and Horsley, 2012), the intestine (Richmond et al., 2015a,b) and even the central nervous system (Cheung and Rando, 2013; Webb et al., 2013; Gilboa and Lehmann, 2004). Unfortunately, quiescent stem cells are also common in cancer and are the bane of chemotherapy; a quiescent cancer stem cell escapes many of the cancer treatments intending to kill the rapidly proliferating cells (Cheung and Rando, 2013; Nakamura-Ishizu et al., 2014). The quiescent cancer stem cells can eventually transition out of quiescence leading to cancer recurrence (Epel, 1967; Pattabiraman and Weinberg, 2014; Tanaka and Dan, 1991). Quiescence in these examples though usually means a slow cell cycle, and sometimes a restriction in transcription. The work presented here though is the first we know of to find quiescence in protein synthesis and in mitochondrial activity *in situ*. In concert with the other quiescent phenotypes found in this same PGC of the sea urchin – cell cycle, transcription, mRNA turnover

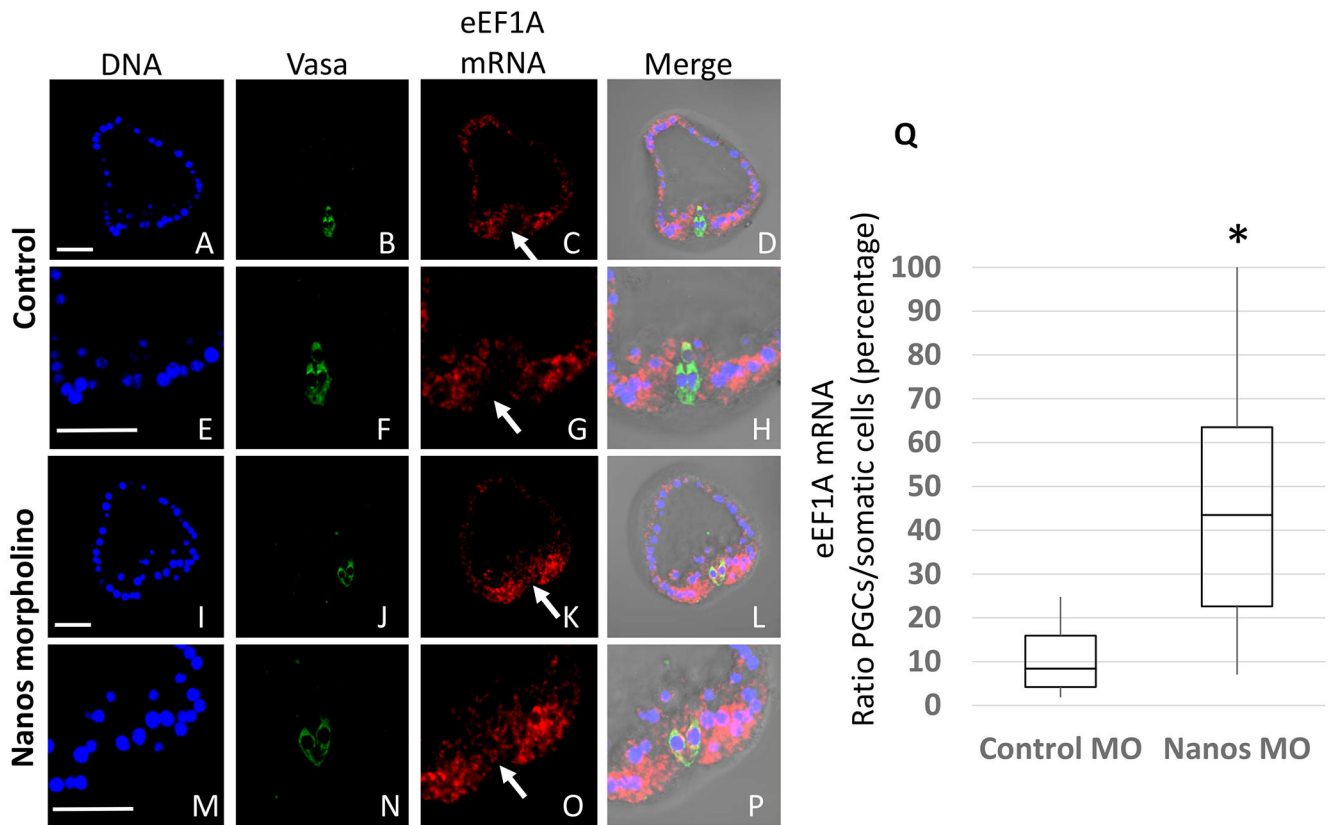


Fig. 4. eEF1A mRNA depletion in the PGCs requires Nanos. (A-P) Fertilized eggs were injected with either a control morpholino or Nanos morpholino, and fixed at blastula stage for eEF1A *in situ* hybridization (red) followed by an immunofluorescence using Vasa antibody (green). DNA was stained with Hoechst (blue). Images are magnified in the area surrounding the PGCs (E-H for the control morpholino; M-P for Nanos morpholino). (Q) The ratio of eEF1A mRNA present in the PGCs versus the somatic cells was quantified using 13 blastulae for the control morpholino and 11 for the Nanos morpholino, and are presented as percentages. The significance of the differences between the control and the Nanos morpholino was assessed using Student's *t*-test (* $P < 0.001$). (A-P) Arrows indicate the PGCs. Approximately 100 embryos were visualized and representative embryos are presented. Scale bars: 20 μ m.

and migration – it serves as an excellent model for how broad cellular activities can be targeted for activation or quiescence with relatively few targets.

The decrease observed here in mitochondrial activity is particularly curious and recently it was found that Hif1 α mRNA is present selectively in the PGCs of this animal at the time of TTQ (Ben-Tabou de-Leon et al., 2013). Hif1 α activity is normally

associated with a transition to glycolysis and although it is not yet known what function, if any, this transcription factor may have in the quiescence phenotype, it is important to consider that its presence in the PGCs is consistent with a shift in metabolism from oxidative phosphorylation towards glycolysis, consistent with the lack of mitochondrial activity in the PGCs; yet this expression is within a normoxic environment. This protein could help explain the

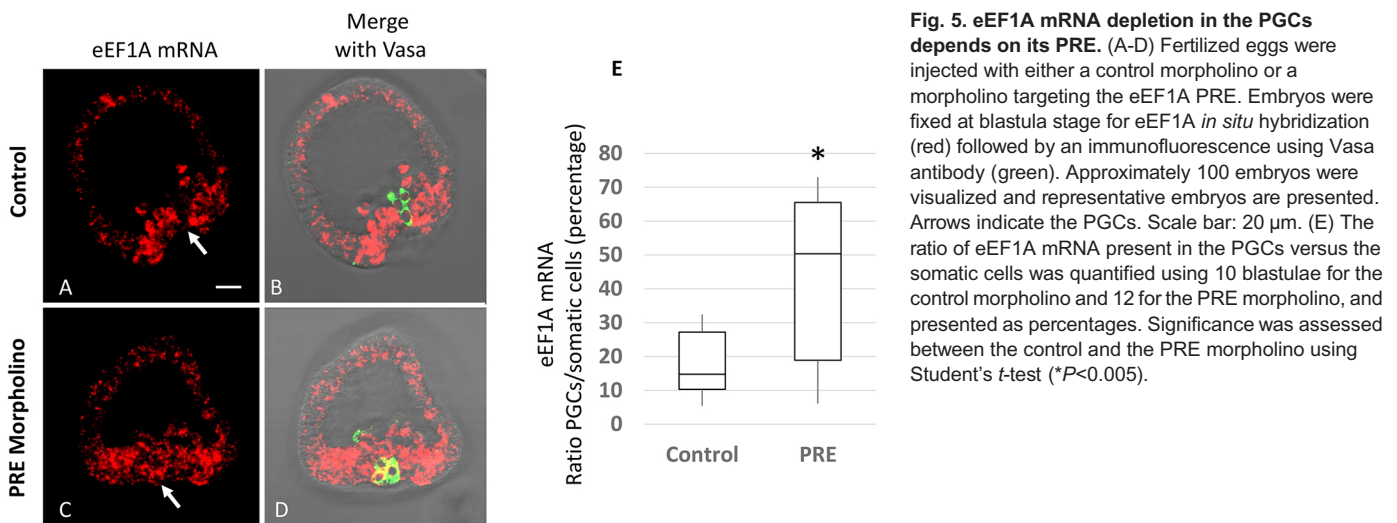


Fig. 5. eEF1A mRNA depletion in the PGCs depends on its PRE. (A-D) Fertilized eggs were injected with either a control morpholino or a morpholino targeting the eEF1A PRE. Embryos were fixed at blastula stage for eEF1A *in situ* hybridization (red) followed by an immunofluorescence using Vasa antibody (green). Approximately 100 embryos were visualized and representative embryos are presented. Arrows indicate the PGCs. Scale bar: 20 μ m. (E) The ratio of eEF1A mRNA present in the PGCs versus the somatic cells was quantified using 10 blastulae for the control morpholino and 12 for the PRE morpholino, and presented as percentages. Significance was assessed between the control and the PRE morpholino using Student's *t*-test (* $P < 0.005$).

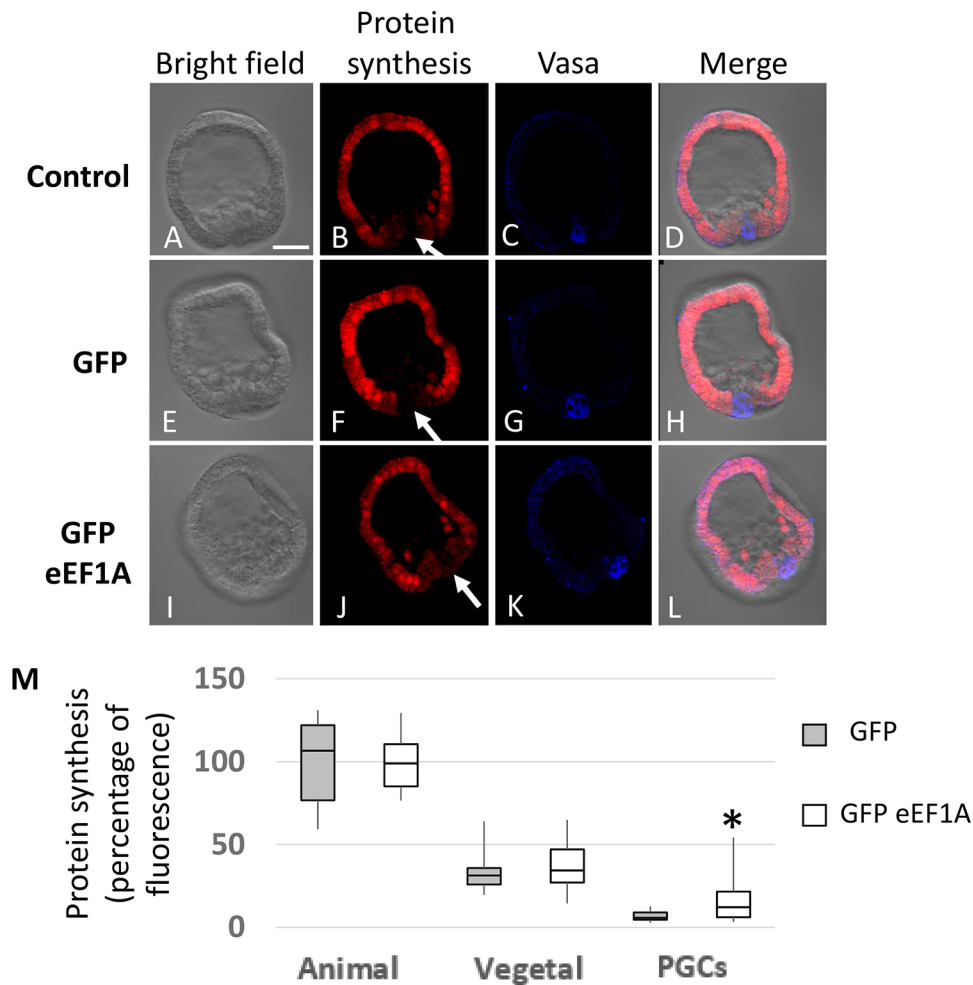


Fig. 6. Overexpression of eEF1A protein specifically increases protein synthesis in the PGCs. (A-L) Fertilized eggs were injected with mRNA coding for either GFP or GFP eEF1A, and treated with OPP at blastula stage before fixation. OPP represents the protein synthesis (red) and Vasa antibody is used to localize the PGCs (blue). Approximately 100 embryos were visualized and representative embryos are presented. Arrows indicate the PGCs. Scale bar: 20 μ m. (M) The protein synthesis in the PGCs and in the somatic cells was quantified using 11 blastulae for GFP, and 16 for GFP eEF1A. Significance was assessed between the GFP and the GFP eEF1A using Student's *t*-test ($*P < 0.05$).

acidification of the PGC by glycolytic activity and perhaps even its developmental fate (López-Iglesias et al., 2015).

The quiescence phenotype of the sea urchin PGCs is transient and, once the PGCs end their quiescence, the cellular activity of these cells appears to start up where they left off. In this animal, the timing of quiescence is from about 6 h post-fertilization, when quiescence begins, to about 72 h, when the PGCs leave quiescence and return to cellular activities that approximate their neighbors to restore transcription, translation, mRNA turnover, protein synthesis, cell cycle and mitochondrial activity. Importantly, the cellular activity and developmental fate of these cells is restored by, and maybe even dependent on, this suspended animation.

How do these PGCs transition out of quiescence? Currently it is not clear, but the turnover of Nanos2 protein and mRNA from the PGC occurs at a time when cellular activity is restored. Therefore, it could be a natural turnover of Nanos2 that restores the cellular activity, but we do not know whether any new transcription or translation of Nanos2 occurs following its initial burst shortly after PGC formation. We are currently working on methods to extend the life of Nanos2 in the PGCs to determine whether the quiescence phenotype is prolonged, and if such persistence has any effect on the cell fate of the PGCs, but we do know that removal of Nanos2 is eventually lethal to the PGCs. Perhaps elevated protein synthesis in the PGCs uses up stored resources generally or the aberrantly translated protein includes overexpression of apoptotic machinery that tips the balance towards cell death. It needs to be kept in mind that Nanos is not the only regulator of the phenotype, so that even

removal of Nanos2 and an increase in protein synthesis (to 47% that of the somatic cells) is sufficient to induce lethality.

Downregulation of general translation machinery is a new mechanism that helps us to understand how PGCs function in this animal, and how quiescence may be manifest. Transcriptome analyses (Swartz et al., 2014) indicate that several RNAs coding for ribosomal proteins are also depleted from the PGCs, which may contribute to the overall 94% decrease in protein synthesis in the PGCs. The 17% increase in newly synthesized proteins when eEF1A is restored suggests that several other factors involved in protein synthesis are also depleted or changed in the PGCs.

MATERIALS AND METHODS

Animals

Strongylocentrotus purpuratus adults were housed in aquaria with artificial seawater (ASW) at 16°C (Coral Life Scientific Grade Marine Salt). Gametes were acquired by either 0.5 M KCl injection or by shaking. Eggs were collected in ASW or filtered seawater and sperm was collected dry. Embryos were cultured in filtered seawater at 16°C.

Nascent protein labeling

Protein synthesis was visualized using the Click-iT protein synthesis assay kit (Life Technologies) with either OPP, O-propargyl-puromycin (C10457) or HPG, L-homopropargylglycine (C10428). Briefly, the embryos were incubated for 30 min with the OPP used at 1:4000, or HPG used at 1:2000, and fixed with PFA 4% in ASW. The nascent proteins were then labeled according to the manufacturer's instructions. At the end of the Click-iT reaction, the embryos were either washed overnight in PBS at 4°C before

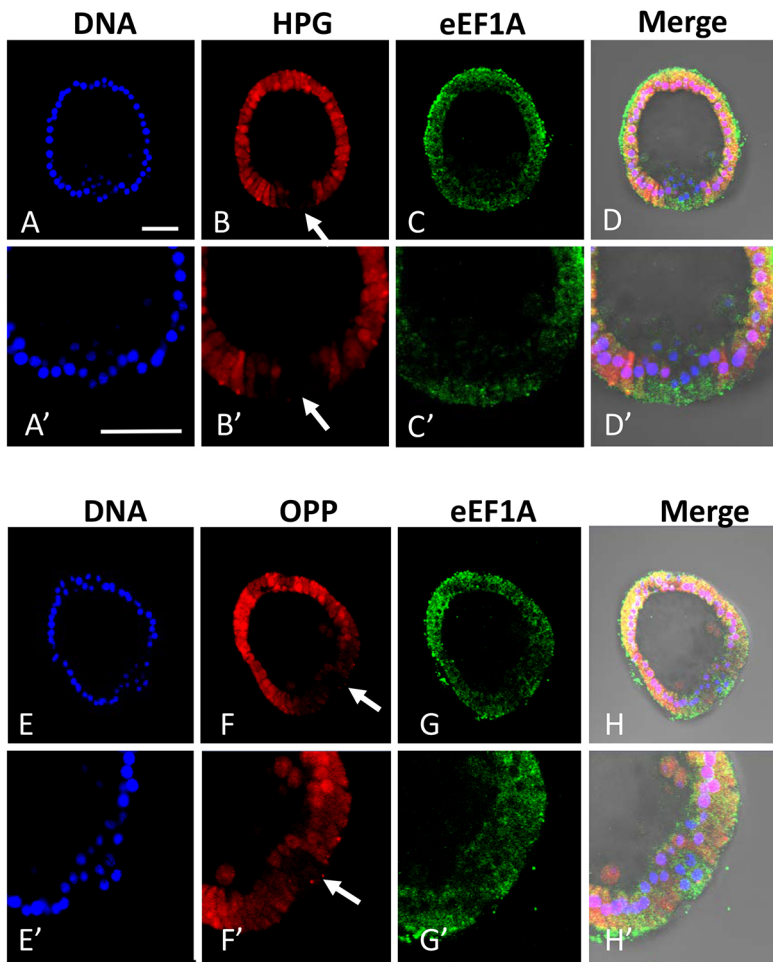


Fig. 7. TTQ starts before the exclusion of eEF1A protein from the PGCs. Early blastulae were treated with either HPG (A-D) or OPP (E-H). After the Click-iT reaction (red), the DNA was stained with Hoechst (blue) and eEF1A protein was followed by immunofluorescence (green). A' to H' are magnifications of the corresponding blastulae (A-H). Approximately 100 embryos were visualized and representative embryos are presented. Arrows indicate the PGCs. Scale bars: 20 μ m.

being imaged, or incubated in the blocking buffer for 1 hour at room temperature, and then incubated with a primary antibody overnight at 4°C for immunofluorescence. Images were captured using a LSM 510 laser scanning confocal microscope (Carl Zeiss) and fluorescence was quantified using Metamorph. For each embryo, three cells were quantified per cell type and averaged into a value representing the protein synthesis per cell type and per embryo. Box and whisker plots of statistical analysis were obtained with Excel (using the minimal, the quartile 1, the median, the quartile 3 and the maximal values).

EdU labeling

The Click-iT EdU Imaging Kit (C10340) was used to label the PGCs (Life Technologies). The modified thymidine analogue EdU is efficiently incorporated into newly synthesized DNA and subsequently fluorescently labeled. Briefly, embryos were soaked in 10 μ M EdU in ASW from fertilization until first cleavage, washed six times with ASW and allowed to develop until the desired stage.

Immunofluorescence

Embryos were cultured as described above and samples were collected at indicated stages of development for whole-mount antibody labeling. Immunofluorescence was carried out as described previously (Juliano et al., 2010). For the Nanos2 antibody (as used by Juliano et al., 2010), embryos were fixed in 4% paraformaldehyde (Electron Microscopy Sciences)/ASW for 10 min at room temperature, extracted in 100% methanol (at -20°C) for 1 min, washed three times with PBS-Tween, and stored at 4°C. For Vasa and eEF1A antibodies (as used by Voronina et al., 2008), embryos were fixed in 4% paraformaldehyde/ASW overnight at 4°C, washed three times with PBS-Tween, and stored at 4°C. Embryos were blocked for 1 h in PBS-Tween, 4% sheep serum and incubated overnight at

4°C with the primary antibody. The *Sp nanos2* affinity-purified antibody (as used by Juliano et al., 2010) was diluted 1:500. The Sp Vasa affinity-purified antibody (as used by Voronina et al., 2008) directed against its N-terminal domain was diluted to 1:200 (Voronina et al., 2008). eEF1A1 antibody (Abcam, ab175274) was used at a dilution of 1:500. For each immunofluorescence, an anti-rabbit Alexa Fluor 488, an anti-rabbit Alexa Fluor 405 or an anti-rabbit Rhodamine was used as the secondary conjugated antibody (Life Technologies), diluted by 1:500 in blocking buffer, for 2 h at room temperature. Images were captured using a LSM 510 laser scanning confocal microscope (Carl Zeiss). Fluorescence was quantified using Metamorph.

Western blot

To test the eEF1A1 antibody, 50 embryos were pelleted for each time point, resuspended in the loading buffer and DTT (Roche; Indianapolis, IN) was added at a final concentration of 5 mM. Samples were incubated at 100°C for 5 min, spun at 14,000 *g* for 2 min, and then loaded onto Tris-glycine, 4-20% gradient gels (Invitrogen). After transfer to nitrocellulose (Pall Corporation), blots were probed with eEF1A1 antibody diluted to 1:2000 in PBS/0.05%Tween/2%BSA. For visualization, blots were probed with an anti-rabbit-HRP secondary antibody diluted 1:5000 in Blotto (Jackson ImmunoResearch Laboratories) and visualized by standard ECL.

Whole-mount *in situ* hybridization

Whole-mount *in situ* hybridization was performed as described previously (Juliano et al., 2006). Approximately 1 kb antisense probe template was PCR amplified from cDNA using a reverse primer tailed with the T7 promoter (lowercase letters in primer sequence). The template for eEF1A probe was amplified using the following primers: F, GGTTCGACAAGCTGAAGG; R, taatcagactactataggAGGGAATCAGTTTGCAATG. The template for

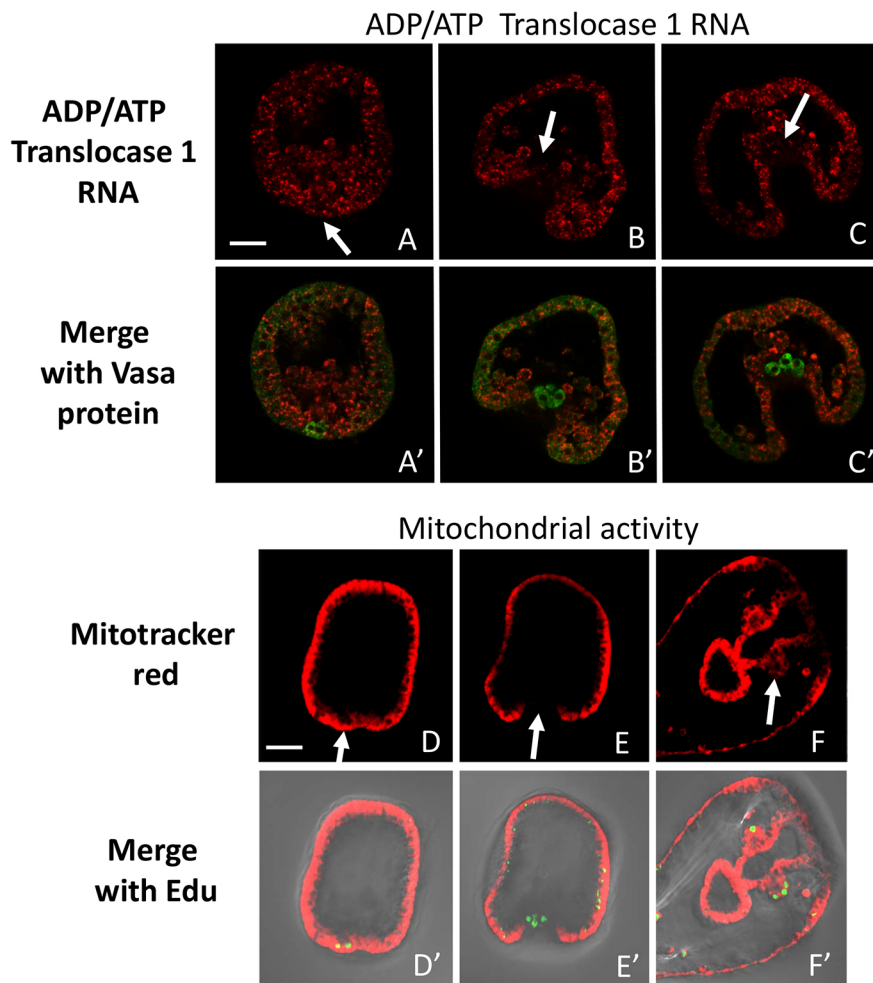


Fig. 8. Mitochondrial activity is reduced in the PGCs. Fluorescent *in situ* hybridization shows that the RNA coding for the ADP/ATP translocase 1 (A-C) is depleted from the PGCs during gastrulation. The embryos were co-labeled using an antibody against Vasa protein (A'-C'). (D-F') Embryos were labeled with Mitotracker red to observe the mitochondrial activity (red) and with Edu (green) to stain the PGCs. Approximately 100 embryos were visualized and representative embryos are presented. Arrows indicate the PGCs. Scale bars: 20 μ m.

the ADP/ATP translocase 1 was amplified using: F, ATGGGCATCGATC-AGGAAGTCGTC; R, taatagactactataggTTAAAATACAAGGAGATTCTTG. Digoxigenin-labeled antisense probes were transcribed using the Roche DIG RNA labeling kit according to the manufacturer's instructions. Embryos were fixed with MOPS-buffered PFA and hybridized for at least 5 days at 50°C with 70% formamide and 0.5 ng/ μ l probe. Hybridization was then visualized using tyramide fluorescence amplification (TSA plus system, PerkinElmer). A non-specific DIG-labeled RNA probe complementary to neomycin-resistance gene (Roche) was used as a negative control.

Microinjections

Microinjections of zygotes were performed as previously described (Cheers and Etensohn, 2004). In brief, eggs were de-jellied with acidic sea water (pH 5.0) for 10 min, washed with filtered sea water three times, lined up with a mouth pipette onto protamine sulfate-coated 60 \times 15 mm petri dishes, fertilized in the presence of 1 mM 3-AT and injected using the Femto Jet injection system (Eppendorf). Glass capillaries (1 \times 90 mm) with filaments (Narishige; Tokyo, Japan) were pulled on a vertical needle puller for injections (Narishige; Tokyo, Japan). Injected embryos were cultured in ASW at 16°C.

Plasmid constructs and RNA *in vitro* synthesis

For the GFP *Sp eEF1A* construct, *Sp eEF1A* ORF was amplified using the following primers surrounded by the *SpeI* restriction site: F1, 5'-cgactagtagtgcctaaaggaaaagcccatatacaatc-3'; R1, 5'-cgactagtagtgccttccttcagcctcttggg-3'. After digestion with *SpeI*, this ORF was cloned into a GFP plasmid (Oulhen et al., 2013) containing *Sp nanos* 5'UTR, GFP ORF followed by *Sp nanos* 3'UTR Δ GNARLE (enabling the accumulation of the RNA in every cell of the blastulae). *Sp eEF1A* ORF was fused to the C

terminal of the GFP ORF. Capped sense RNAs were synthesized using the mMessage mMachine T7 Kit (Ambion) yielding RNA concentrations between 0.5 and 2 μ g/ μ l. Injection solutions contained 20% glycerol with 1×10^{12} copies of a GFP RNA. Approximately 2 μ l of each RNA mixture (<5% of egg volume) was injected into each fertilized egg.

Morpholino approach

Morpholinos against *Sp nanos2* (gtgactaaagtgcgtgaaactcga) (Juliano et al., 2010) and against the PRE of *Sp eEF1A* (catacactgtttccattacatac) were purchased from Gene Tools. *Sp Nanos2* morpholino was injected at 500 μ M stock concentration and *Sp eEF1A* PRE morpholino was injected at 1 mM stock concentration. Morpholino injection solutions include 20% glycerol and 1 mM 10,000 MW dextran conjugated to Texas Red (Life Technologies). A non-relevant morpholino against the sea star *Patiria miniata dysferlin* (5'-tcgacacaatcaccatcagcgacat-3') was used as a control.

CRISPR/Cas9 approach

The plasmid pCS2-3xFLAG-NLS-*SpCas9*-NLS (a gift from Yonglong Chen, Chinese Academy of Sciences; Addgene plasmid #51307) was linearized with *NcoI* and transcribed with SP6. Four gRNA templates directed against *Sp Nanos2* were designed according to CRISPRscan priorities (CRISPRscan.org): *Sp nanos2.190* (taatagactactataGGTGACTGGCTCGTCGAGACgttttagactagaa), *Sp nanos2.250* (taatagactactataGGGATCTCAGCGATGTTCAGgttttagactagaa), *Sp nanos2.295* (taatagactactataGGAGGAAGGC-GAGCCAACAgttttagactagaa) and *Sp nanos2.319* (taatagactactata-gGAGGTGGTGCTACGGGTGgttttagactagaa). The gRNAs were synthesized by T7 RNA polymerase using the MegaShortScript T7 transcription kit (AM1354, ThermoFisher) and purified using the miRNeasy mini kit (217004) (Qiagen). These RNAs were mixed

(400 ng/μl of each gRNA and 500 ng/μl of Cas9 mRNA), injected into freshly fertilized eggs and cultured as described previously (Cheers and Etensohn, 2004). The genomic DNA of injected embryos was extracted with 10 μl of QuickExtract DNA Extraction Solution (<http://www.epibio.com/>), according to the manufacturer's instructions.

Mitochondria analysis

The abundance of the mitochondria was tested using the MitoTracker Green FM (M7514, ThermoFisher Scientific): a green-fluorescent mitochondrial stain that appears to localize to mitochondria regardless of mitochondrial membrane potential. The mitochondrial activity was observed using the MitoTracker Red CMXRos (M7512, ThermoFisher Scientific): a red fluorescent dye, the accumulation of which depends upon the membrane potential. For each stage, embryos were incubated with 200 nM of MitoTracker green or MitoTracker Red for 15 min at 16°C.

Acknowledgements

We thank the members of PrIMO for a rich work environment. We thank Dr Thomas Onorato for initially exposing us to the new Click-IT technologies and Geoff Williams for imaging assistance.

Competing interests

The authors declare no competing or financial interests.

Author contributions

N.O. and G.M.W. designed the experiments and wrote the paper. N.O. injected morpholinos and RNAs, measured translational activity with OPP and HPG, and tested the mitochondrial activity. S.Z.S. and J.L. did the *in situ* hybridization for eEF1A RNA. J.L. tested the eEF1A antibody. A.M. helped to test and quantify the quiescence in the PGCs.

Funding

We gratefully acknowledge the National Institutes of Health (R01HD028152 to G.M.W.). Deposited in PMC for release after 12 months.

Supplementary information

Supplementary information available online at <http://dev.biologists.org/lookup/doi/10.1242/dev.144170.supplemental>

References

- Ahringer, J. and Kimble, J. (1991). Control of the sperm-oocyte switch in *Caenorhabditis elegans* hermaphrodites by the fem-3 3' untranslated region. *Nature* **349**, 346-348.
- Asaoka-Taguchi, M., Yamada, M., Nakamura, A., Hanyu, K. and Kobayashi, S. (1999). Maternal Pumilio acts together with Nanos in germline development in *Drosophila* embryos. *Nat. Cell Biol.* **1**, 431-437.
- Ben-Tabou de-Leon, S., Su, Y.-H., Lin, K.-T., Li, E. and Davidson, E. H. (2013). Gene regulatory control in the sea urchin aboral ectoderm: spatial initiation, signaling inputs, and cell fate lockdown. *Dev. Biol.* **374**, 245-254.
- Boonsanay, V., Zhang, T., Georgieva, A., Kostin, S., Qi, H., Yuan, X., Zhou, Y. and Braun, T. (2016). Regulation of skeletal muscle stem cell quiescence by Suv4-20h1-dependent facultative heterochromatin formation. *Cell Stem Cell* **18**, 229-242.
- Brandhorst, B. P. (1976). Two-dimensional gel patterns of protein synthesis before and after fertilization of sea urchin eggs. *Dev. Biol.* **52**, 310-317.
- Cheers, M. S. and Etensohn, C. A. (2004). Rapid microinjection of fertilized eggs. *Methods Cell Biol.* **74**, 287-310.
- Cheung, T. H. and Rando, T. A. (2013). Molecular regulation of stem cell quiescence. *Nat. Rev. Mol. Cell Biol.* **14**, 329-340.
- Cho, P. F., Gamberi, C., Cho-Park, Y. A., Cho-Park, I. B., Lasko, P. and Sonenberg, N. (2006). Cap-dependent translational inhibition establishes two opposing morphogen gradients in *Drosophila* embryos. *Curr. Biol.* **16**, 2035-2041.
- Cormier, P., Pyronnet, S., Morales, J., Mulner-Lorillon, O., Sonenberg, N. and Bellé, R. (2001). eIF4E association with 4E-BP decreases rapidly following fertilization in sea urchin. *Dev. Biol.* **232**, 275-283.
- Dalby, B. and Glover, D. M. (1993). Discrete sequence elements control posterior pole accumulation and translational repression of maternal cyclin B RNA in *Drosophila*. *EMBO J.* **12**, 1219-1227.
- Davidson, E. H. (1976). *Gene Activity in Early Development*. New York: Academic Press.
- Epel, D. (1967). Protein synthesis in sea urchin eggs: a "late" response to fertilization. *Proc. Natl. Acad. Sci. USA* **57**, 899-906.
- Fukada, S., Uezumi, A., Ikemoto, M., Masuda, S., Segawa, M., Tanimura, N., Yamamoto, H., Miyagoe-Suzuki, Y. and Takeda, S. (2007). Molecular signature of quiescent satellite cells in adult skeletal muscle. *Stem Cells* **25**, 2448-2459.
- Gilboa, L. and Lehmann, R. (2004). Repression of primordial germ cell differentiation parallels germ line stem cell maintenance. *Curr. Biol.* **14**, 981-986.
- Goldstein, J. and Horsley, V. (2012). Home sweet home: skin stem cell niches. *Cell. Mol. Life Sci.* **69**, 2573-2582.
- Hayashi, Y., Hayashi, M. and Kobayashi, S. (2004). Nanos suppresses somatic cell fate in *Drosophila* germ line. *Proc. Natl. Acad. Sci. USA* **101**, 10338-10342.
- Irish, V., Lehmann, R. and Akam, M. (1989). The *Drosophila* posterior-group gene nanos functions by repressing hunchback activity. *Nature* **338**, 646-648.
- Juliano, C. E., Voronina, E., Stack, C., Aldrich, M., Cameron, A. R. and Wessel, G. M. (2006). Germ line determinants are not localized early in sea urchin development, but do accumulate in the small micromere lineage. *Dev. Biol.* **300**, 406-415.
- Juliano, C. E., Yajima, M. and Wessel, G. M. (2010). Nanos functions to maintain the fate of the small micromere lineage in the sea urchin embryo. *Dev. Biol.* **337**, 220-232.
- Kadyrova, L. Y., Habara, Y., Lee, T. H. and Wharton, R. P. (2007). Translational control of maternal Cyclin B mRNA by Nanos in the *Drosophila* germline. *Development* **134**, 1519-1527.
- Karp, G. C. and Weems, M. D. (1975). 3H-amino acid uptake and incorporation in sea urchin gastrulae and exogastrulae: an autoradiographic study. *J. Exp. Zool.* **194**, 535-545.
- Lai, F., Zhou, Y., Luo, X., Fox, J. and King, M. L. (2011). Nanos1 functions as a translational repressor in the *Xenopus* germline. *Mech. Dev.* **128**, 153-163.
- Lai, F., Singh, A. and King, M. L. (2012). *Xenopus* Nanos1 is required to prevent endoderm gene expression and apoptosis in primordial germ cells. *Development* **139**, 1476-1486.
- López-Iglesias, P., Alcaina, Y., Tapia, N., Sabour, D., Arauzo-Bravo, M. J., Sainz de la Maza, D., Berra, E., O'Mara, A. N., Nistal, M., Ortega, S. et al. (2015). Hypoxia induces pluripotency in primordial germ cells by HIF1 alpha stabilization and Oct4 deregulation. *Antioxid. Redox Signal.* **22**, 205-223.
- Merrick, W. C. A. N. J. (2000). *The Protein Biosynthesis Elongation Cycle*. Cold Spring Harbor, NY, Cold Spring Harbor Laboratory Press.
- Morales, J., Mulner-Lorillon, O., Cosson, B., Morin, E., Bellé, R., Bradham, C. A., Beane, W. S. and Cormier, P. (2006). Translational control genes in the sea urchin genome. *Dev. Biol.* **300**, 293-307.
- Morris, R. J., Liu, Y., Marles, L., Yang, Z., Trempus, C., Li, S., Lin, J. S., Sawicki, J. A. and Cotsarelis, G. (2004). Capturing and profiling adult hair follicle stem cells. *Nat. Biotechnol.* **22**, 411-417.
- Murata, Y. and Wharton, R. P. (1995). Binding of pumilio to maternal hunchback mRNA is required for posterior patterning in *Drosophila* embryos. *Cell* **80**, 747-756.
- Nakamura-Ishizu, A., Takizawa, H. and Suda, T. (2014). The analysis, roles and regulation of quiescence in hematopoietic stem cells. *Development* **141**, 4656-4666.
- Oulhen, N. and Wessel, G. M. (2016). Albinism as a visual, in vivo guide for CRISPR/Cas9 functionality in the sea urchin embryo. *Mol. Reprod. Dev.* **83**, 1046-1047.
- Oulhen, N., Yoshida, T., Yajima, M., Song, J. L., Sakuma, T., Sakamoto, N., Yamamoto, T. and Wessel, G. M. (2013). The 3'UTR of nanos2 directs enrichment in the germ cell lineage of the sea urchin. *Dev. Biol.* **377**, 275-283.
- Pattabiraman, D. R. and Weinberg, R. A. (2014). Tackling the cancer stem cells - what challenges do they pose? *Nat. Rev. Drug Discov.* **13**, 497-512.
- Rezza, A., Sennett, R. and Rendl, M. (2014). Adult stem cell niches: cellular and molecular components. *Curr. Top. Dev. Biol.* **107**, 333-372.
- Richmond, C. A., Shah, M. S., Carlone, D. L. and Breault, D. T. (2015a). Factors regulating quiescent stem cells: Insights from the intestine and other self-renewing tissues. *J. Physiol.* **13**, 2403-2411.
- Richmond, C. A., Shah, M. S., Deary, L. T., Trotier, D. C., Thomas, H., Ambruzs, D. M., Jiang, L., Whites, B. B., Rickner, H. D., Montgomery, R. K. et al. (2015b). Dormant intestinal stem cells are regulated by PTEN and nutritional status. *Cell Rep.* **13**, 2403-2411.
- Sato, K., Hayashi, Y., Ninomiya, Y., Shigenobu, S., Arita, K., Mukai, M. and Kobayashi, S. (2007). Maternal Nanos represses hid/skl-dependent apoptosis to maintain the germ line in *Drosophila* embryos. *Proc. Natl. Acad. Sci. USA* **104**, 7455-7460.
- Sonoda, J. and Wharton, R. P. (1999). Recruitment of Nanos to hunchback mRNA by Pumilio. *Genes Dev.* **13**, 2704-2712.
- Starck, S. R., Green, H. M., Alberola-Ila, J. and Roberts, R. W. (2004). A general approach to detect protein expression in vivo using fluorescent puromycin conjugates. *Chem. Biol.* **11**, 999-1008.
- Swartz, S. Z., Reich, A. M., Oulhen, N., Raz, T., Milos, P. M., Campanale, J. P., Hamdoun, A. and Wessel, G. M. (2014). Deadenylase depletion protects inherited mRNAs in primordial germ cells. *Development* **141**, 3134-3142.

- Tanaka, S. and Dan, K.** (1991). Study of the lineage and cell cycle of small micromeres in embryos of the sea urchin, *Hemicentrotus pulcherrimus*. *Dev. Growth Differ* **32**, 145-156.
- Valcourt, J. R., Lemons, J. M. S., Haley, E. M., Kojima, M., Demuren, O. O. and Collier, H. A.** (2012). Staying alive: metabolic adaptations to quiescence. *Cell Cycle* **11**, 1680-1696.
- Voronina, E., Lopez, M., Juliano, C. E., Gustafson, E., Song, J. L., Extavour, C., George, S., Oliveri, P., McClay, D. and Wessel, G.** (2008). Vasa protein expression is restricted to the small micromeres of the sea urchin, but is inducible in other lineages early in development. *Dev. Biol.* **314**, 276-286.
- Webb, A. E., Pollina, E. A., Vierbuchen, T., Urbán, N., Ucar, D., Leeman, D. S., Martynoga, B., Sewak, M., Rando, T. A., Guillemot, F. et al.** (2013). FOXO3 shares common targets with ASCL1 genome-wide and inhibits ASCL1-dependent neurogenesis. *Cell Rep.* **4**, 477-491.
- Wessel, G. M., Brayboy, L., Fresques, T., Gustafson, E. A., Oulhen, N., Ramos, I., Reich, A., Swartz, S. Z., Yajima, M. and Zazueta, V.** (2014). The biology of the germ line in echinoderms. *Mol. Reprod. Dev.* **81**, 679-711.
- Wharton, R. P. and Struhl, G.** (1991). RNA regulatory elements mediate control of *Drosophila* body pattern by the posterior morphogen nanos. *Cell* **67**, 955-967.
- Williamson, A. and Lehmann, R.** (1996). Germ cell development in *Drosophila*. *Annu. Rev. Cell Dev. Biol.* **12**, 365-391.
- Wreden, C., Verrotti, A. C., Schisa, J. A., Lieberfarb, M. E. and Strickland, S.** (1997). Nanos and pumilio establish embryonic polarity in *Drosophila* by promoting posterior deadenylation of hunchback mRNA. *Development* **124**, 3015-3023.
- Zhang, B., Gallegos, M., Puoti, A., Durkin, E., Fields, S., Kimble, J. and Wickens, M. P.** (1997). A conserved RNA-binding protein that regulates sexual fates in the *C. elegans* hermaphrodite germ line. *Nature* **390**, 477-484.

Supplemental Information

Test of reagent specificity using control embryos

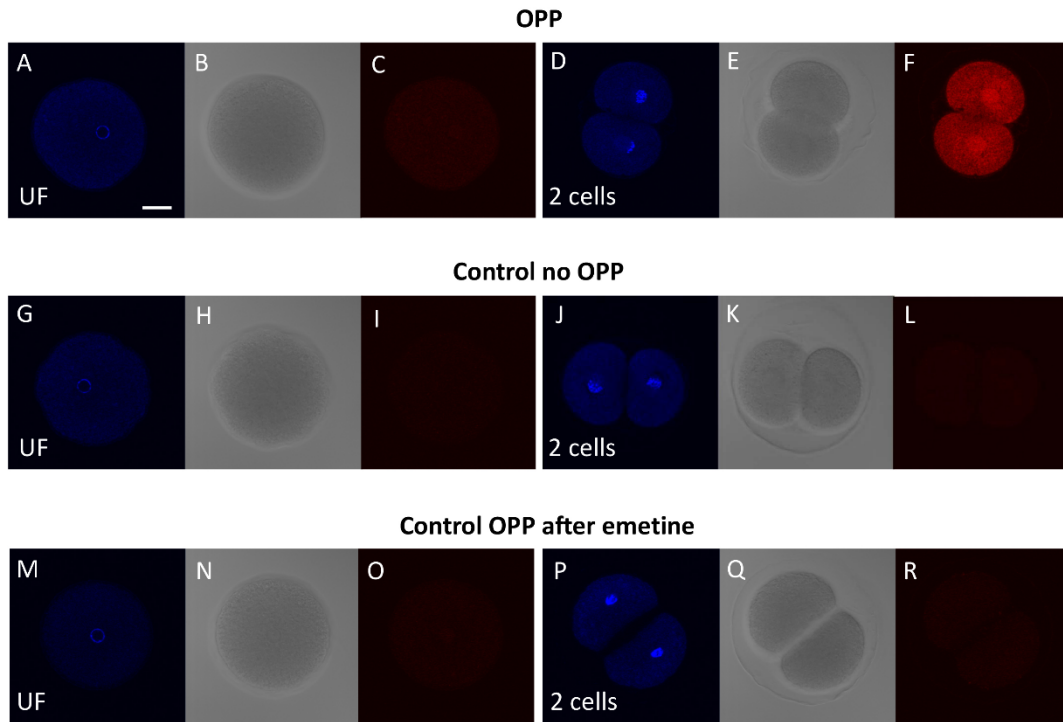


Figure S1: OPP specifically labels protein synthesis in sea urchin embryos. Unfertilized eggs, UF (A,B,C) and 2 cell stage embryos (D,E,F) were incubated with OPP. For each stage, controls are shown using no OPP (G to L), or using OPP in presence of 1mM emetine (M to R), a translational inhibitor. After the click it reaction, protein synthesis was only detected in the 2 cell stage embryos treated with OPP. Approximately one hundred embryos were visualized and representative embryos are presented. Scale bar, 20 μm .

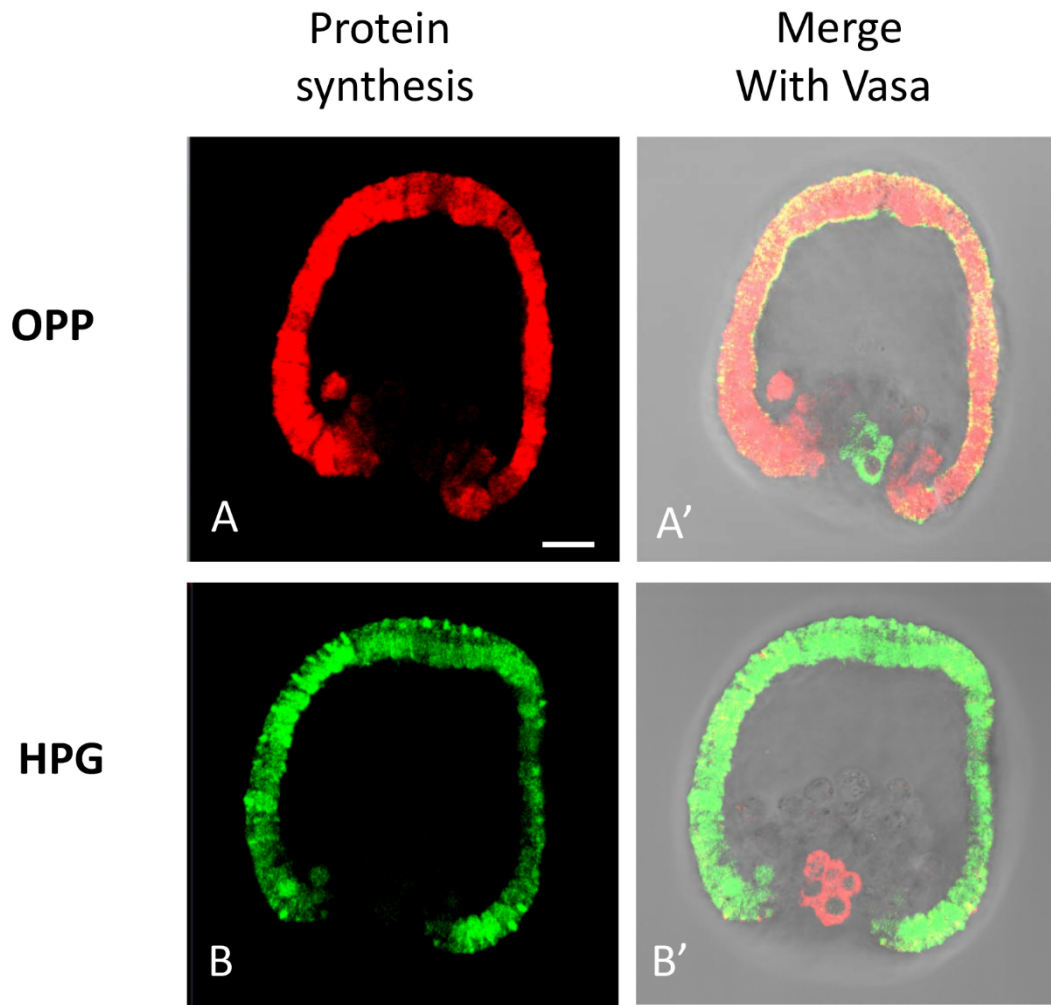


Figure S2: Protein synthesis, measured with OPP and HPG, is reduced in the PGCs. Embryos at blastula stage were treated with either OPP (red in A and A') or HPG (green in B and B') for 30 minutes. After the Click-iT reaction and the vasa immunofluorescence (green in A' and red in B'), embryos were imaged. Protein synthesis is barely detectable in the PGCs. Approximately one hundred embryos were visualized and representative embryos are presented. Arrows indicate the PGCs. Scale bar, 20 μ m.

Anti Sp Nanos

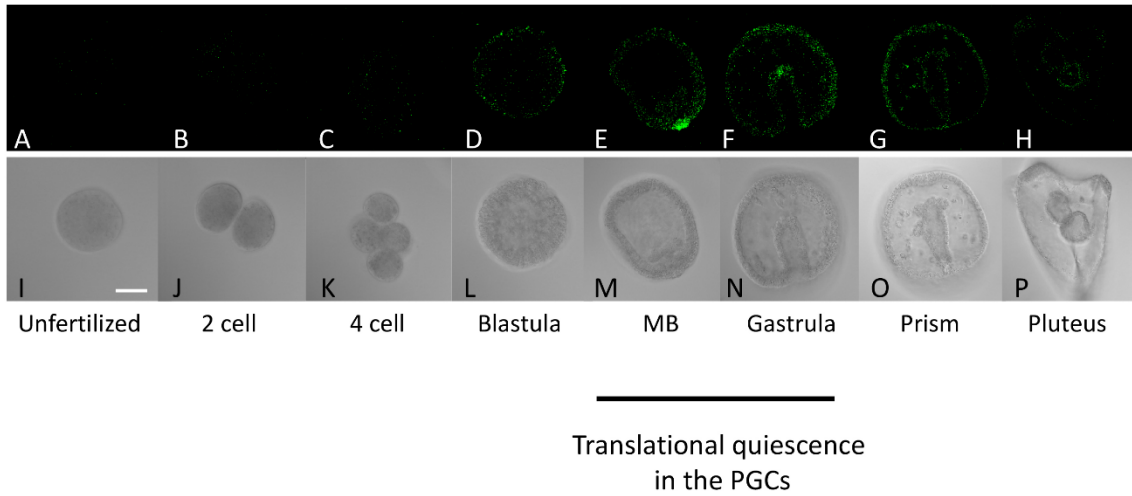


Figure S3: Expression of *Sp Nanos2* protein during the early development of the sea urchin embryos. Immunofluorescence using *Sp Nanos 2* antibody (A to H). Images were taken using the same microscope settings (laser intensity, pin-hole opening) at 400x magnification. The corresponding brightfield images are shown from I to P. Approximately one hundred embryos were visualized and representative embryos are presented. Arrows indicate the PGCs. Scale bar, 20 μ m.

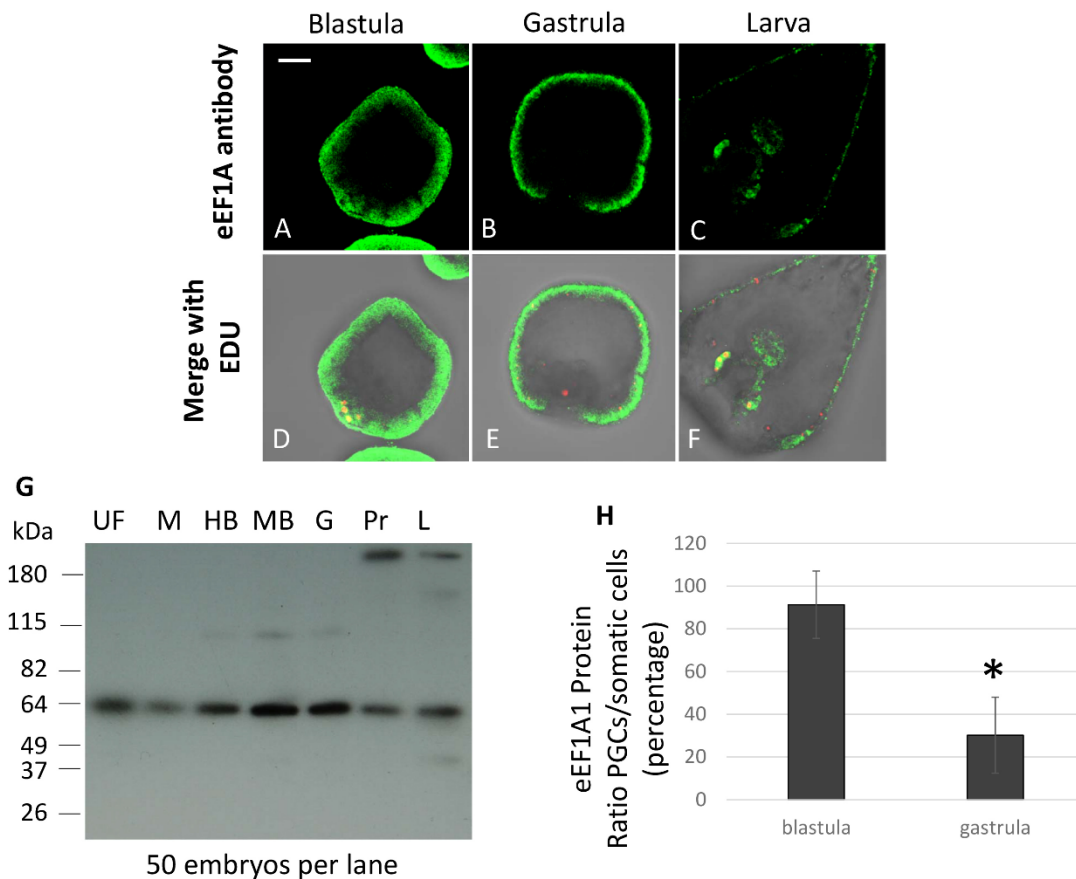


Figure S4: eEF1A protein is transiently excluded from the PGCs between blastula and early gastrula development. Embryos were fixed at different time points to test the expression of the protein eEF1A during the development. Using an antibody against eEF1A, the immunofluorescence shows the exclusion of the eEF1A protein (green) from the PGCs labelled with Edu (red). By Western blot (G), the antibody recognizes one main protein band in unfertilized eggs (UF), morula (M), hatched blastula (HB), mesenchyme blastula (MB), gastrula (G), prism (Pr) and 3 day larvae (L). The immunofluorescences (A, B, C) were used to quantify (H) the eEF1A protein exclusion from the PGCs compared to the somatic cells using 9 blastulae and 13 gastrulae. Significance was assessed Student *t* test ($P < 0.001$). Approximately one hundred embryos were visualized and representative embryos are presented. Scale bar, 20 μ m.

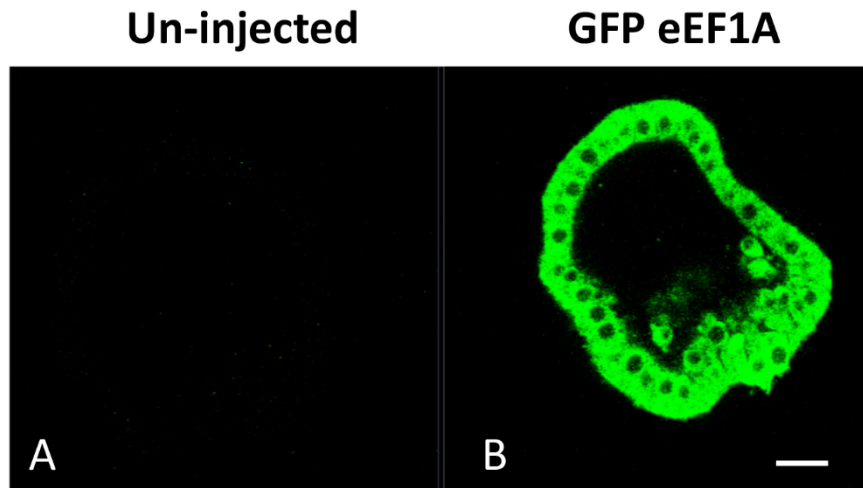


Figure S5: The protein GFP eEF1A is expressed throughout the blastula. An mRNA coding for a GFP eEF1A fused to a 3'UTR lacking the PRE was injected in fertilized eggs. The expression of the GFP eEF1A was observed at the blastula stage (B). Un-injected blastulae were used as a control (A). Scale bar, 20 μ m.

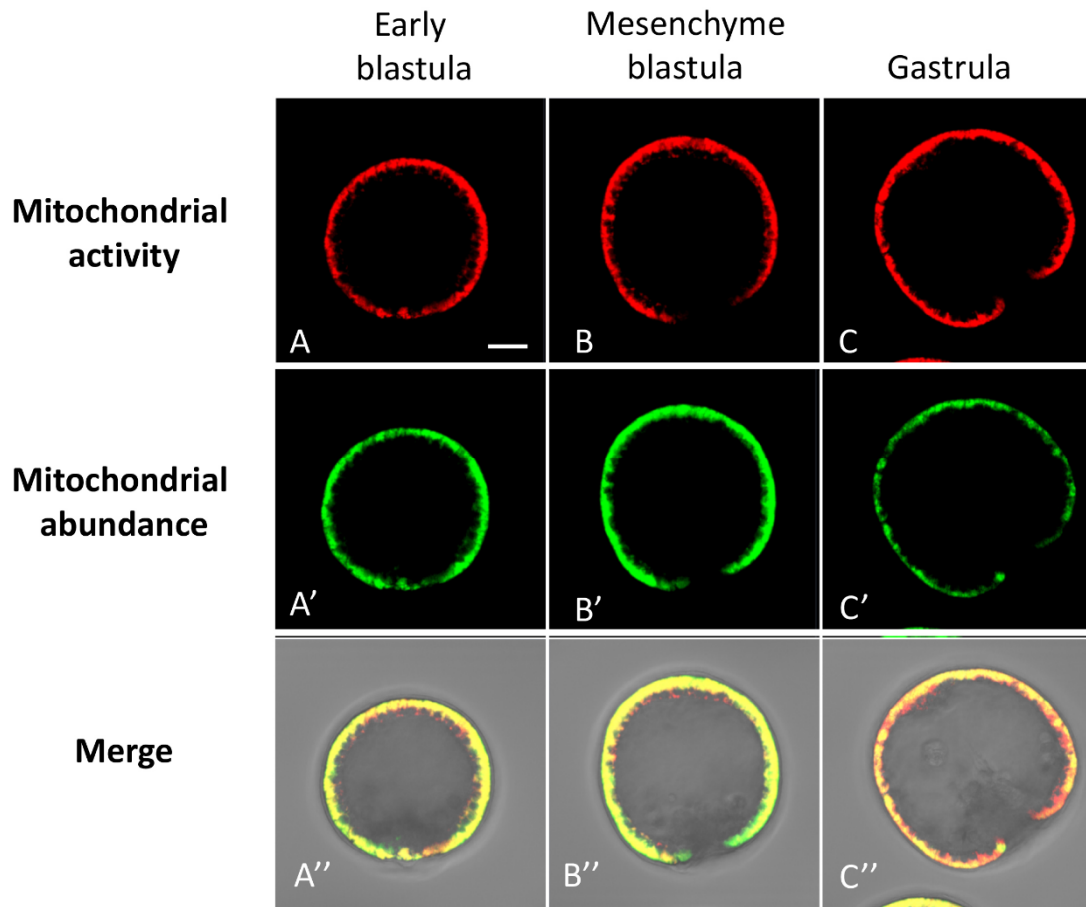


Figure S6: Mitochondrial activity is reduced in the PGCs. Embryos were co-labelled with Mitotracker red and Mitotracker green. Both mitochondrial activity (A to C), and mitochondrial abundance (A' to C') are reduced in the PGCs. A, A' and A'' represent the same embryo. Approximately one hundred embryos were visualized and representative embryos are presented. Scale bar, 20 μ m.

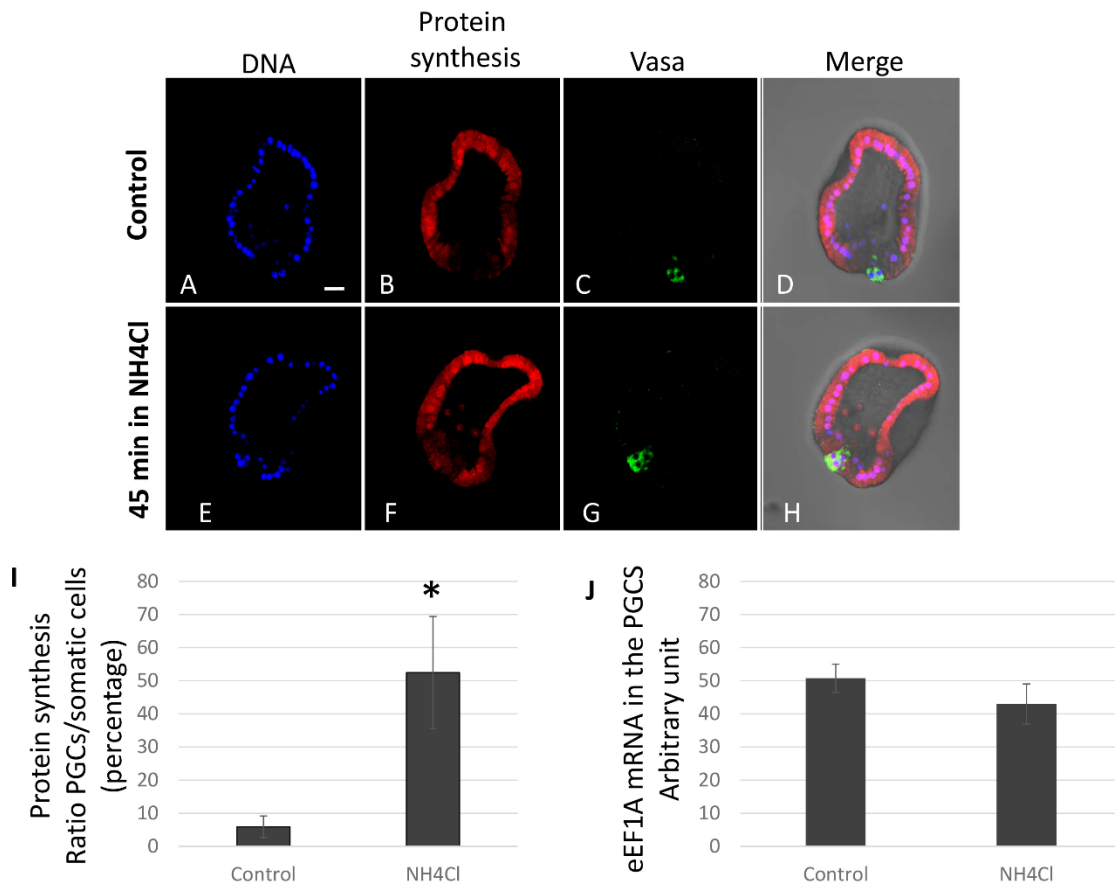


Figure S7: The transient translational quiescence is pH dependent. Blastulae were treated with 10mM NH₄Cl pH8 for 45 minutes, OPP was added after 15 minutes of treatment, for an additional 30 minute co-incubation with NH₄Cl. Control blastulae were cultured in absence of NH₄Cl, but were also treated with OPP. The nuclei are represented in blue (Hoechst), protein synthesis in red, and vasa immunofluorescence in green. The ratio of OPP between the PGCs and the somatic cells was quantified using 11 blastulae for the control, and 12 for the NH₄Cl treatment (I). Significance was assessed between the control and the NH₄Cl treated embryos with the use of Student *t* test ($P < 0.001$). The level of eEF1A mRNA was also quantified in the PGCs, in the presence or absence of NH₄Cl (J). No statistical significance was detected in the eEF1A mRNA levels between control and ammonium chloride treated embryos. Approximately one hundred embryos were visualized and representative embryos are presented. Scale bar, 20 μ m. between blastula and gastrula with the use of